PAPER Special Section on Microwave and Millimeter-Wave Technologies

120-W Ku-Band GaN SSPA with Diode Linearizer for Future Broadcasting Satellites

Masafumi NAGASAKA[†a)], **Masaaki KOJIMA**[†], **Takuma TORII**[††], ***Members***,
Hiromitsu UTSUMI[†††], ***Nonmember***, **Koji YAMANAKA**[†††], **Shintaro SHINJO**[††],
Mitsuhiro SHIMOZAWA[††], ***Senior Members***, ***and*** **Hisashi SUJIKAI**[†], ***Member***

SUMMARY Satellite broadcasting of 4K/8K ultra-high definition television (UHDTV) was launched in Japan in December 2018. Because this system uses the amplitude and phase shift keying (APSK) modulation scheme, there is a need to improve the non-linear characteristics of the satellite transponders. To meet this requirement, we have been developing a 120-W-class Ku-band solid state power amplifier (SSPA) as a replacement for the currently used traveling wave tube amplifier (TWTA). In this study, we developed a gallium-nitride (GaN) SSPA and linearizer (LNZ). The SSPA achieved an output power of 120 W while maintaining a power added efficiency (PAE) of 31%. We evaluated the transmission performance of 16APSK in this SSPA channel in comparison with that in the TWTA channel.

key words: *broadcasting satellite, SSPA, Ku-band, GaN*

1. Introduction

Broadcasting services such as 4K/8K ultra-high definition television (UHDTV) are attracting attention all over the world [1]. In Japan, the Ministry of Internal Affairs and Communications has issued a road map that calls for UHDTV satellite broadcasting [2]. UHDTV satellite broadcasting services were launched in December 2018.

Ku-band traveling wave tube amplifiers (TWTAs) have been used in satellite transponders for providing satellite broadcasting in Japan, because of their high output power. The TWTA operation requires converting the spacecraft bus voltages into several kilovolts with an electronic power conditioner (EPC), and the total weight of the typical Ku-band TWTA and EPC is 1.8 kg [3]. Therefore, solid state power amplifiers (SSPAs) have an advantage to mitigate the operating voltage and weight and have been studied as replacements for TWTAs in the lower frequency bands [4]. It is also expected that SSPAs will replace TWTAs operating in the Ku-Band. As for the signal amplified in the satellite, a transmission standard for UHDTV satellite broadcasting (ISDB-S3) has been recommended by ITU-R [5], which deals with modulation schemes of amplitude and phase shift keying (APSK) to increase the transmission capacity. TWTAs need to be operated at a large back-off to reduce their non-linearities when APSK signals are transmitted.

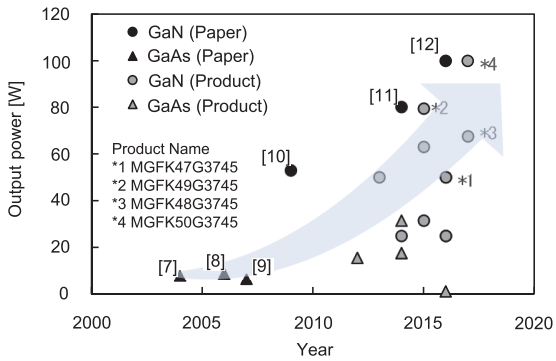

Fig. 1 Trend in Ku-band PAs.

In general, SSPAs have better linearity than TWTAs [6]. However, the efficiency and output power of SSPAs fabricated with gallium-arsenide (GaAs) technology have not yet reached the levels of TWTAs. Recently, the chances of obtaining high efficiency and high output power from SSPAs have increased because of the development of gallium-nitride (GaN) devices. Figure 1 shows the trend of Ku-band power amplifiers (PAs). From 2004 to 2006, 10-W-class devices had been built from GaAs [7]–[9]. In 2009, a GaN PA with an output power of over 50 W under continuous wave (CW) conditions was developed [10]. Since 2014, GaN technology has been used to achieve 80-W-class output powers [11], [12]. A 120-W-class SSPA applying this technology could be a replacement for the 120-W-class TWTA in the current broadcasting satellite transponder [13]. So far, we have studied using 100-W-class SSPAs for a broadcasting satellite operating in the 12-GHz band (11.7 to 12.2 GHz) [14]–[16].

In this paper, we describe a 120-W-class 12-GHz-band SSPA. The SSPA comprises a diode linearizer (LNZ), GaN driver amplifier (DA), and GaN high power amplifier (HPA). The HPA achieves an output power of 120 W (50.8 dBm). In designing SSPAs, un-modulated signals are typically used as the input signal; for example, a LNZ is tuned with a two-tone signal (two un-modulated-signals). However, we cannot evaluate the transmission performance of APSK signals accurately with these methods. Therefore, we designed and evaluated our SSPA with the 16APSK used for UHDTV satellite broadcasting in Japan. In Sect. 2, we describe the

Manuscript received January 31, 2019.
Manuscript revised May 24, 2019.

[†]The authors are with NHK Science & Technology Research Laboratories, Japan Broadcasting Corporation, Tokyo, 157–8510 Japan.
[††]The authors are with Mitsubishi Electric Corporation, Information Technology R&D Center, Kamakura-shi, 247–8501 Japan.
[†††]The authors are with Mitsubishi Electric Corporation, High Frequency & Optical Device Works, Itami-shi, 664–8641 Japan.
a) E-mail: nagasaka.m-hm@nhk.or.jp

DOI: 10.1587/transele.2019MMP0006

satellite transponder model, evaluation methods, and definitions for designing the SSPA. Sections 3 and 4 describe the design and performance of the SSPA. Section 5 discusses the transmission performance of 16APSK in SSPA channels. We summarize the paper in Sect. 6.

2. Transmission Model for Broadcasting Satellite

It is important to evaluate the transmission performance over the whole satellite loopback to develop a 120-W-class SSPA because the radio frequency (RF) components of the satellite transponder, which includes amplifiers and filters, impact digital signals. Below, we describe the satellite channel model and the methods used in our evaluation.

2.1 Satellite Channel Model

Figure 2 shows the block diagram of the satellite channel model in our simulation, which is mainly made up of a transmitter, satellite transponder, and receiver. The dashed line in the figure outlines the configuration of a typical satellite transponder, which consists of an input multiplexer (IMUX) filter, a TWTA, and an output multiplexer (OMUX) filter [17], [18]. The role of the satellite transponder is to filter a single carrier out of the uplink signals, amplify it, and send it to the service area.

The specifications of the modulated signal for our evaluation are listed in Table 1. A 16APSK (FEC code rate: 7/9) signal in accordance with ISDB-S3 (Nyquist bandwidth: 33.7561 MHz, roll-off factor: 0.03) is transmitted from the mapper in Fig. 2, because 16APSK is used in 4K/8K UHDTV satellite broadcasting in Japan. The "EQ." block in the receiver means an adaptive equalizer based on the least-squares-error criterion [19].

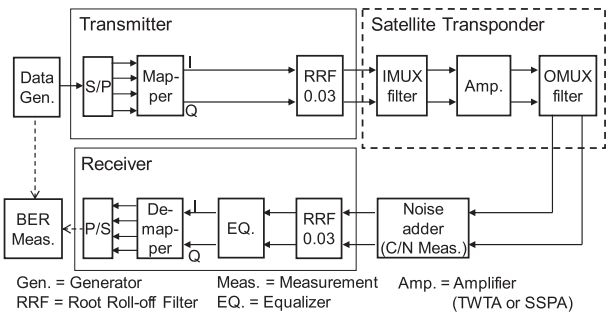

Fig. 2 Block diagram of satellite channel model in our simulations.

Table 1 Specifications of modulated signal.

Modulation scheme (FEC code rate)		16APSK (7/9)
Symbol rate		33.7561 Mbaud
Occupied bandwidth		34.5 MHz
Roll-off factor		0.03
FEC	Inner code	LDPC (code length: 44880)
	Outer code	BCH (65535, 65343) shortened code

FEC: Forward Error Correction

Figure 3 shows the AM/AM and AM/PM characteristics of the TWTA, which are actual measurements from indoor tests [17]–[19]. In the case of the 120-W-class TWTA, the normalized output power of 0 dB corresponds to 120 W (50.8 dBm). It is desirable for the TWTA to amplify the signal as much as possible and have maximum output power, because a 45-cm-diameter parabolic reflector antenna is used for reception of the satellite broadcasting [20]. Therefore, the TWTA is operated near the saturation point. On the other hand, the transmission performance deteriorates in saturated operation because of the increase in non-linearity. Thus, there is a trade-off between the gain of the amplifier and the linearity.

Figure 4 shows the amplitude and group delay characteristics of the IMUX and OMUX filters, which are also actual measurements from the indoor tests [17]–[19]. The role of the IMUX is to filter a single carrier out of the other adjacent broadcasting waves [21]. The role of the OMUX is to suppress spectrum re-growth induced by operating the TWTA near the saturation point [6]. To play these roles, the non-uniform group delays within the Nyquist band of the IMUX and OMUX filters remain. These characteristics negatively impact transmission performance [22]. Therefore, it is necessary to evaluate the transmission performances of the TWTA and SSPA under the same IMUX and OMUX characteristics. We used the characteristics of Fig. 4 as common parameters in the simulations of Sects. 3.4 and 4.2 and in the experiments in Sect. 5.

2.2 Definition of OBO

The output back-off (OBO) in the simulations and experi-

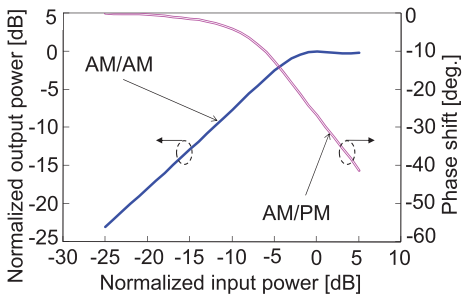

Fig. 3 AM/AM and AM/PM characteristics of TWTA.

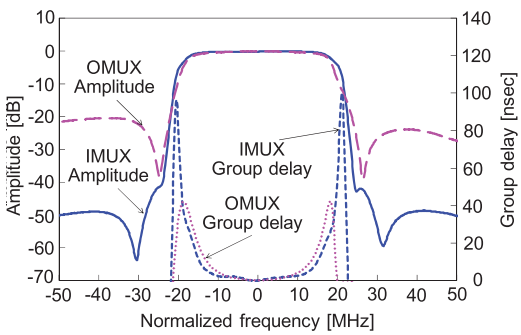

Fig. 4 Amplitude and group delay characteristics of IMUX and OMUX filters (central frequency: 12.03436 GHz (BS-17ch) normalized to 0 Hz).

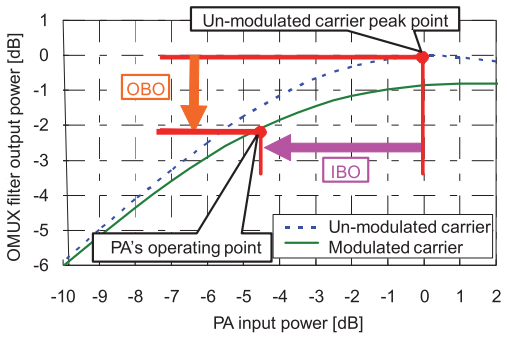

Fig. 5 Input back-off (IBO) and output back-off (OBO) definitions.

ments was defined as the ratio of the OMUX filter output power of the un-modulated carrier peak point to that of the modulated carrier operating point [23], as shown in Fig. 5.

2.3 Evaluation Methods

We can increase availability of broadcasting services by improving the transmission performance. The performance can be evaluated using the total degradation, which is the value of the required carrier to noise power ratio (C/N) + OBO. The OBO results in a decrease in received C/N when considering the link budget, which means a decrease in the link margin. Therefore, the most advantageous transmission is when the required C/N + OBO is a minimum. We quantitatively evaluated the transmission performance by comparing the required C/N + OBO in simulations and experiments. The definitions of the required C/N are described below.

The required C/N in the experiments was defined as the C/N at a bit error rate (BER) of 1×10^{-11} with forward error correction (FEC) [23]. Its value was derived from an extrapolation of three measurement points in the C/N versus BER characteristics [23]. In the simulations, the required C/N was also defined as the C/N at the BER of 1×10^{-11} and derived as follows [24]:

A) The C/N at a BER of 1×10^{-11} for 16APSK (7/9) at the ideal loopback with FEC is 10.8 dB [23].
B) The BER for 16APSK (7/9) at the ideal loopback without FEC is 4.94×10^{-2}, when the C/N is 10.8 dB.
C) From A) and B), we can say that the C/N at a BER of 4.94×10^{-2} at the satellite loopback without FEC is the required C/N because it equals the C/N at the BER of 1×10^{-11} with FEC.

3. SSPA Design and HPA Prototype

3.1 Configuration of SSPA

Figure 6 shows the configuration of the SSPA prototype. The SSPA mainly includes a diode linearizer (LNZ), GaN driver amplifier (DA), and GaN high power amplifier (HPA). The LNZ compensates for the AM/AM and AM/PM distortion of the whole PAs [16]. The DA has a saturation power

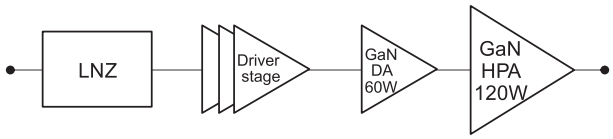

Fig. 6 Configuration of SSPA prototype.

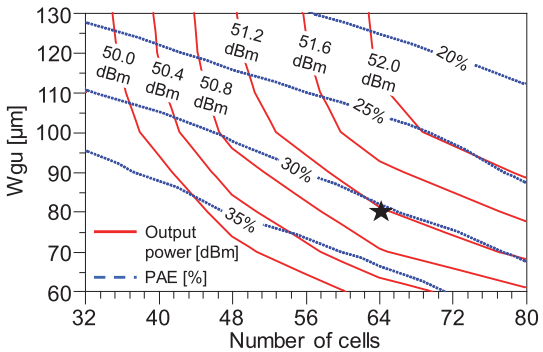

Fig. 7 Estimated performance of HPA.

of 60 W and has been reported in detail [15].

In this section, we describe the 120-W HPA prototype and verify its transmission performance. The HPA has the following requirements:

1. Output power up to 120 W (50.8 dBm).
2. Better transmission performance for 16APSK (7/9) than when using the TWTA in Fig. 3.

3.2 Design of HPA

The output power of the HPA becomes higher when a device size characteristic such as the unit gate width (Wgu) becomes larger [15], [16]. In order to increase the output power, the whole transistor needs to be enlarged. There are two methods of enlarging the transistor. One is to enlarge Wgu. However, in so doing, the power density and gain are decreased, and thus, the maximum power is limited and power added efficiency (PAE) is also decreased. The other method is to increase the number of cells. However, the combiner loss is increased in this case, and thus, there is a trade-off between the output power and PAE. For this reason, we optimized the size of the transistor to obtain an output power of 120 W with high efficiency. We calculated the output power and PAE of the HPA depending on Wgu and the number of cells while considering this trade-off.

Figure 7 shows the estimated performance of the HPA. The output power and PAE are estimated under the conditions of a power density variation of 0.12 dB per Wgu of 10 μm and gain variation of 0.3 dB per Wgu of 10 μm. The region over 50.8 dBm of output power and 30% of PAE for 64 cells is the largest at a Wgu from 70 to 80 μm. Hence, we set Wgu to 80 μm and used 64cells to have a margin of output power obtaining 30% of PAE. To achieve a higher PAE, we used a second harmonic reflection circuit [15] and set the gate length at 0.15 μm.

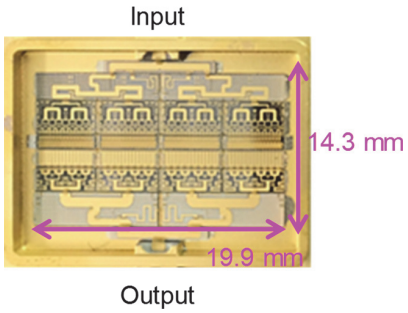

Fig. 8 Photograph of HPA prototype.

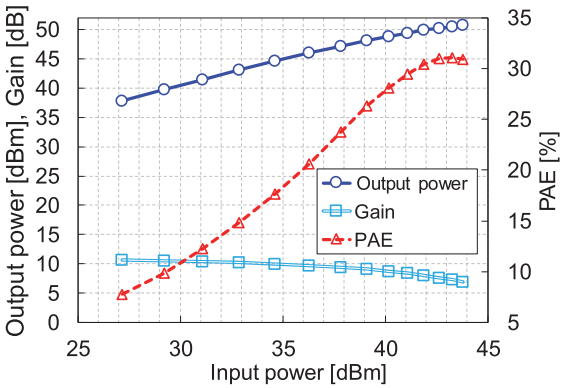

Fig. 9 Measured output performance of HPA (CW frequency: 12.0 GHz, drain bias voltage: 30 V).

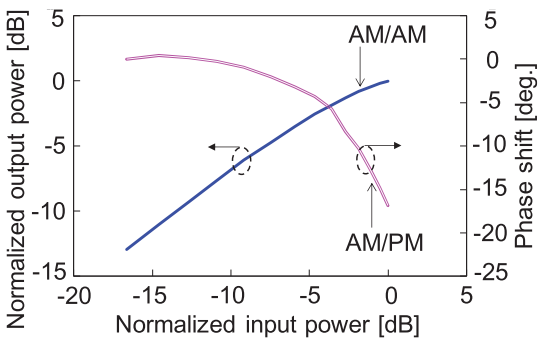

Fig. 10 Measured AM/AM and AM/PM characteristics of HPA.

3.3 HPA Prototype

Figure 8 shows the HPA prototype that we fabricated based on the design in Sect. 3.2, and Fig. 9 shows the measured output performance. The output power resulted in 120 W (50.8 dBm) when the PAE and gain were 31% and 7 dB, respectively. Figure 10 shows the measured AM/AM and AM/PM characteristics for the prototype. Here, the normalized input and output powers at the peak point in Fig. 10 (both 0 dB) correspond to 43.8 and 50.8 dBm, respectively. Figure 11 shows the recent trend of GaN PAs in the Ku band. To the best of our knowledge, this is the first time that an output power of 120 W has been reported for devices operating in the Ku-band.

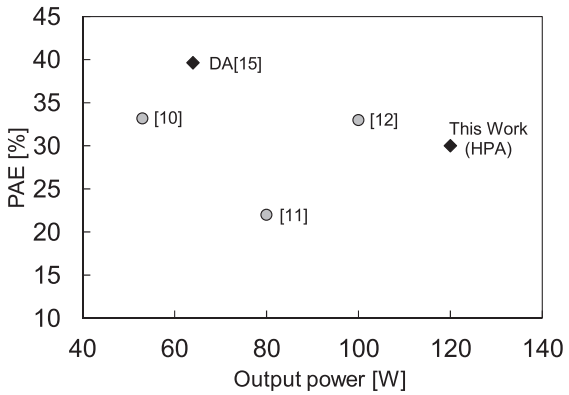

Fig. 11 State-of-the-art GaN PAs operating in Ku band.

Table 2 Simulation results of required C/N + OBO for 16APSK (7/9) (TWTA versus HPA systems).

	Channel	IBO [dB]	OBO [dB]	Required C/N [dB]	Required C/N + OBO [dB]
A)	IMUX – TWTA – OMUX	4.43	2.20	12.49	14.69
B)	IMUX – SSPA (HPA) – OMUX	2.50	2.20	12.39	14.59

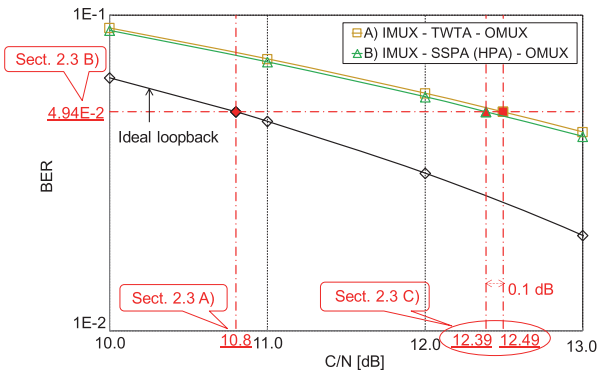

Fig. 12 C/N versus BER characteristics for 16APSK (7/9) without FEC at satellite loopback in simulations (total bits: 10^6): A) IMUX filter – TWTA – OMUX filter [IBO = 4.43 dB, OBO = 2.20 dB], B) IMUX filter – SSPA (HPA) – OMUX filter [IBO = 2.50 dB, OBO = 2.20 dB].

3.4 Simulated Transmission Performance of HPA

To verify requirement B) in Sect. 3.1, we simulated the transmission performance for 16APSK (7/9) through the HPA prototype. We calculated the required C/N in steps A) – C) of Sect. 2.3. A block diagram of the simulation is shown in Fig. 2. We compared the TWTA and HPA systems in terms of the following channel models:

A) IMUX filter (Fig. 4) – TWTA (Fig. 3) – OMUX filter (Fig. 4)
B) IMUX filter – SSPA (HPA) (Fig. 10) – OMUX filter

The OBOs for channels A) and B) were fixed to 2.2 dB [13], and the input back-off (IBO) was derived from the OBO. Figure 12 shows the C/N versus BER characteristics for 16APSK (7/9) without FEC over channels A) and B). This figure also indicates the values for the ideal loop-

back, described in Sect. 2.3. Table 2 lists the total degradations in terms of the required C/N + OBOs obtained from Fig. 12. The total degradation for HPA system B) was 0.1 dB smaller than that for TWTA system A). From these simulation results, we confirmed that the transmission performance of our HPA prototype is equivalent to the TWTA. Thus, in the next section, we describe the design of a LNZ, which connects to the HPA, to improve performance.

4. Linearizer Design and Prototype

We developed a 12-GHz-band LNZ to compensate for distortion due to the amplifier characteristics (AM/AM and AM/PM) of the HPA prototype described in Sect. 3. We did not consider the LNZ to compensate for the distortion due to the group delay characteristics in Fig. 4. The required C/N + OBO can be decreased by connecting the LNZ to the HPA, as shown in Fig. 6. The configuration of the LNZ and how its parameters are optimized are described below.

4.1 Design of LNZ

Figure 13 shows the equivalent circuit of the LNZ. We can compensate for the AM/AM and AM/PM characteristics by using diodes. However, the AM/PM variation in the 12-GHz band is limited by parasitic inductances between the diode and ground. To reduce the parasitic inductances, we used the topology of a diode linearizer with a virtual ground [25]. The input signal is separated into two paths, the phases of which differ by 180 degrees (Fig. 13). Accordingly, a virtual short is generated at the center of diode. Therefore, the effect of the parasitic inductance becomes negligible.

4.2 LNZ Parameter Study with Simulated Transmission Performance

The linearity of a PA depends on the shape of the AM/AM and AM/PM characteristics. We compared several characteristics corresponding to the LNZ parameters in simulations for the LNZ, DA, and HPA connected in series like in Fig. 6. Here, we utilized the characteristics of the DA and HPA as the measurements and assumed that there were four micro strip line (MSL) lengths in the LNZ for tuning. Figure 14 shows the simulated AM/AM, normalized gain, and AM/PM characteristics of the SSPA (LNZ–DA–HPA) for LNZs with four different MSL lengths.

To select the MSL length (0.5, 1.0, 1.5, or 2.0 mm), we evaluated the transmission performance for 16APSK (7/9) through the LNZs. We calculated the required C/Ns in steps A) – C) in Sect. 2.3 in the same way as in Sect. 3.4. A block diagram of the simulation is shown in Fig. 2. The following channel models were compared:

A) IMUX filter (Fig. 4) – SSPA (LNZ (MSL length: 0.5 mm) – DA – HPA) (Fig. 14) – OMUX filter (Fig. 4)
B) IMUX filter – SSPA (LNZ (MSL length: 1.0 mm) – DA – HPA) – OMUX filter

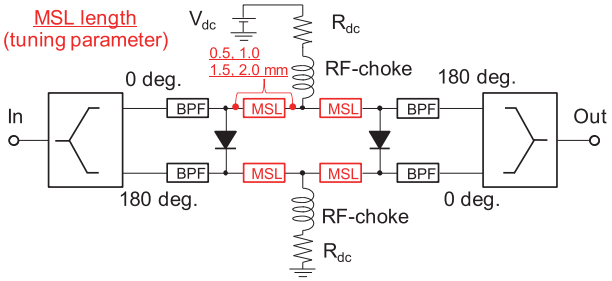

Fig. 13 Equivalent circuit of LNZ.

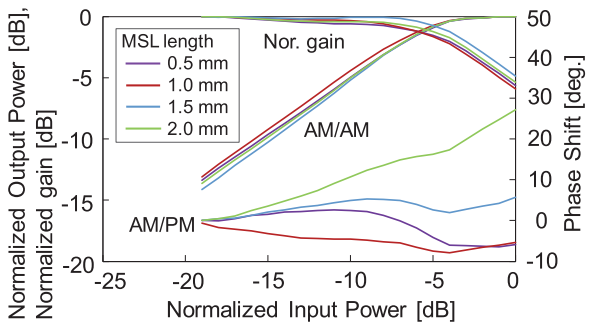

Fig. 14 Simulated AM/AM, normalized gain, and AM/PM characteristics of SSPA (LNZs (MSL length: 0.5, 1.0, 1.5, 2.0 mm) – DA – HPA).

Table 3 Simulation results of required C/N + OBOs for 16APSK (7/9) (four different LNZs).

	Channel	IBO [dB]	OBO [dB]	Required C/N [dB]	Required C/N + OBO [dB]
A)	IMUX – SSPA (LNZ (0.5 mm) – DA – HPA) – OMUX	5.28	2.20	11.95	14.15
B)	IMUX – SSPA (LNZ (1.0 mm) – DA – HPA) – OMUX	5.65	2.20	11.92	14.12
C)	IMUX – SSPA (LNZ (1.5 mm) – DA – HPA) – OMUX	5.28	2.20	11.85	14.05
D)	IMUX – SSPA (LNZ (2.0 mm) – DA – HPA) – OMUX	5.32	2.20	12.02	14.22

C) IMUX filter – SSPA (LNZ (MSL length: 1.5 mm) – DA – HPA) – OMUX filter
D) IMUX filter – SSPA (LNZ (MSL length: 2.0 mm) – DA – HPA) – OMUX filter

The OBOs from channels A) to D) are 2.2 dB [13]. Table 3 lists the total degradations in terms of the required C/N + OBOs in simulations in the same way as in Sect. 3.4. System C) (MSL length: 1.5 mm) performed the best because the required C/N + OBO for it was 14.05 dB. We chose this MSL length for the LNZ hardware.

4.3 LNZ Prototype

Figure 15 shows a photograph of the 12-GHz-band LNZ prototype. The substrate is composed of alumina. The diodes are implemented on the transmission lines. Figure 16 shows the measured AM/AM and AM/PM characteristics of the SSPA (LNZ – DA – HPA) which had an LNZ with a 1.5-mm-long MSL. Here, the normalized input (LNZ input) and

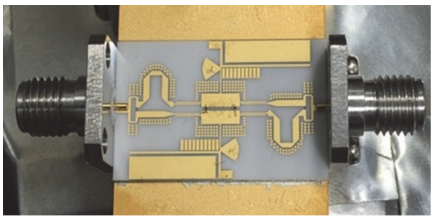

Fig. 15 Photograph of LNZ prototype.

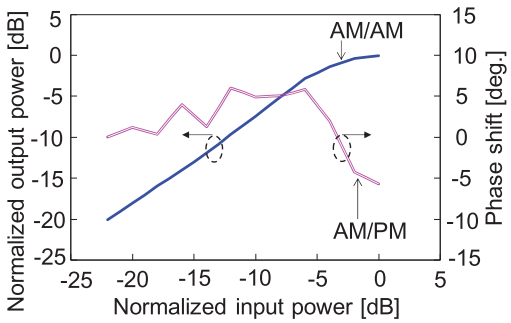

Fig. 16 Measured AM/AM and AM/PM characteristics of SSPA (LNZ – DA – HPA).

output (HPA output) powers at the peak point in Fig. 16 correspond to −5.0 and 50.8 dBm, respectively. We used this SSPA model in the experiments described in Sect. 5.

5. Transmission Experiments

5.1 Experimental System

Figure 17 shows a block diagram of the transmission system of our experiments. The dashed line marks the area of the 12-GHz-band satellite transponder in the satellite simulator composed of hardware [17]–[19]. We conducted transmission tests by replacing the TWTA with the SSPA inside this satellite simulator and evaluated the differences in transmission performance in the following channel models:

A) IMUX filter (Fig. 4) – TWTA (Fig. 3) – OMUX filter (Fig. 4)
B) IMUX filter – SSPA (Fig. 16) – OMUX filter

The OBOs of A) and B) were controlled by a variable attenuator at the IMUX filter output and set to 2.2 dB [13].

The center frequency of the modulated carrier from the transmitter was 140 MHz. The satellite simulator consisted of a frequency up-converter (from 140 MHz to 12.03436 GHz), 12-GHz-band satellite transponder (satellite channel), and frequency down-converter (from 12.03436 GHz to 140 MHz). The modulated signal over the satellite simulator went into a noise adder for the downlink C/N measurement.

5.2 Experimental Results

Figure 18 shows the C/N versus BER characteristics for 16APSK (7/9). Table 4 lists the required C/N + OBO obtained from Fig. 18. The required C/N + OBO for 16APSK

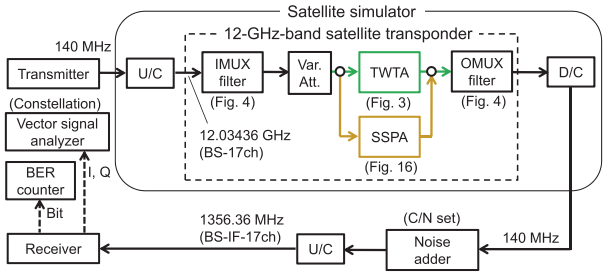

Fig. 17 Block diagram of experimental transmission system.

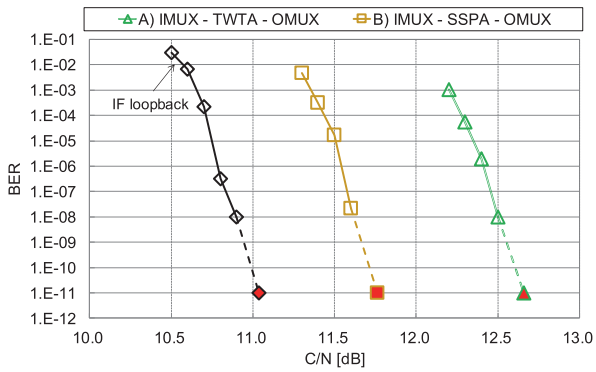

Fig. 18 C/N versus BER for 16APSK (7/9) with FEC at satellite loopback in experiments (total bits: 10^{10}): A) IMUX filter – TWTA – OMUX filter [OBO = 2.2 dB], B) IMUX filter – SSPA – OMUX filter [OBO = 2.2 dB].

Table 4 Experimental results of required C/N + OBO for 16APSK (7/9) for TWTA and SSPA systems.

Channel	OBO [dB]	Required C/N [dB]	Required C/N + OBO [dB]
IMUX – TWTA – OMUX	2.2	12.7	14.9
IMUX – SSPA – OMUX	2.2	11.8	14.0

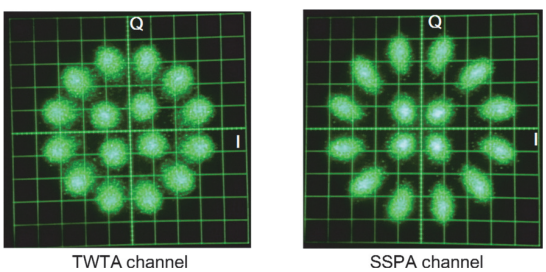

Fig. 19 Received constellations for 16APSK (7/9) at OBO of 2.2 dB.

(7/9) was 14.9 dB at channel A), whereas it was 14.0 dB at channel B). Under the same OBO of 2.2 dB for both channels, the required C/N + OBO improved by 0.9 dB as a result of using the developed SSPA.

Figure 19 shows the received constellations without downlink noise for 16APSK (7/9) at channels A) and B). The constellation at B) (SSPA) rotated less than at A) (TWTA). From these constellations, it can be seen that the phase shift of the SSPA, which depends on the input power, is smaller than that of the TWTA.

6. Conclusion

We fabricated a 120-W 12-GHz-band SSPA prototype with a diode linearizer for improving 4K/8K satellite broadcasting services in the future. We evaluated its transmission performance in simulations to determine the design parameters for the fabrication process and in experiments as a final test. What we obtained from this study are as follows.

- The fabricated HPA achieved a 120-W output power with a PAE of 31%. This is the highest output power yet reported for a single GaN HPA in the 12-GHz band.
- We developed a 12-GHz-band LNZ. We designed it by making an evaluation using the 16APSK signal of ISDB-S3 rather than an un-modulated or two-tone signal. This method is the first such attempt in this field.
- We conducted transmission experiments showing that the transmission performance of 16APSK (7/9) in the SSPA channel improved by 0.9 dB compared with that in the TWTA channel in operation at an OBO of 2.2 dB.

Acknowledgments

This research was performed under the auspices of a program called "Research and Development of Technology Encouraging Effective Utilization of Frequency for Ultra-high-definition Satellite and Terrestrial Broadcasting System" funded by the Ministry of Internal Affairs and Communications, Japan.

References

[1] ITU-R, "Parameter values for ultra-high definition television systems for production and international programme exchange," Recommendation ITU-R BT.2020, Oct. 2015.
[2] The ITU Association of Japan, "Promoting the advancement of broadcasting services: the road map to 4K and 8K," ITU-AJ New Breeze, vol.26, no.2, Spr. 2014.
[3] L3 Technologies, Electron devices products. Available: https://www2.l3t.com/edd/products/index.htm
[4] K. Osawa, H. Yoshikoshi, A. Nitta, T. Tanaka, E. Mitani, and T. Satoh, "High-Efficiency L-Band 200-W GaN HEMT for Space Applications," SEI technical review, vol.191, pp.32–37, July 2017 (in Japanese).
[5] ITU-R, "Transmission system for UHDTV satellite broadcasting," Recommendation ITU-R BO.2098, Dec. 2016.
[6] S. Tirró, "Satellite communication systems design," New York, the United States, Springer, 1993.
[7] Q. Zhang and S.A. Brown, "Fully monolithic 8 watts Ku-band high power amplifier," 2004 MTT-S International Microwave Symposium Digest (IEEE Cat. No.04CH37535), pp.1159–1162, 2004.
[8] C.H. Lin, H.Z. Liu, C.K. Chu, H.K. Huang, Y.H. Wang, C.C. Liu, C.H. Chang, C.L. Wu, and C.S. Chang, "A fully matched Ku-band 9W pHEMT MMIC high power amplifier," Proc. IEEE Compound Semicond. Integr. Circuits Symp., San Antonio, the United States, pp.165–168, Nov. 2006.
[9] C.-H. Lin, H.-Z. Liu, C.-K. Chu, H.-K. Huang, C.-C. Liu, C.-H. Chang, C.-L. Wu, C.-S. Chang, and Y.-H. Wang, "A compact 6.5-W pHEMT MMIC power amplifier for Ku-band applications," Microwave Wireless Components Lett., vol.17, no.2, pp.154–156, March 2007.
[10] K. Takagi, S. Takatsuka, Y. Kashiwabara, S. Teramoto, K. Matsushita, H. Sakurai, K. Onodera, H. Kawasaki, Y. Takada, and K. Tsuda, "Ku-band AlGaN/GaN-HEMT with over 30% of PAE," MTT'09. IEEE MTT-S International Microwave Symposium Digest, pp.457–460, June 2009.
[11] S. Imai, H. Maehara, M. Koyanagi, H. Ohtsuka, A. Ohta, K. Yamanaka, A. Inoue, and H. Fukumoto, "An 80-W packaged GaN high power amplifier for CW operation in the 13.75–14.5 GHz band," Proc. 2014 IEEE MTT-S International Microwave Symposium, Tampa, the United States, pp.1–4, June 2014.
[12] T. Torii, S. Imai, H. Maehara, M. Miyashita, T. Kunii, T. Morimoto, A. Inoue, A. Ohta, H. Katayama, N. Yunoue, K, Yamanaka, and H. Fukumoto, "60% PAE, 30W X-band and 33% PAE, 100W Ku-band PAs utilizing 0.15 μm GaN HEMT technology," Proc. 46th European Microwave Conference (EuMC), London, the United Kingdom, pp.568–571, Oct. 2016.
[13] M. Kojima, Y. Suzuki, M. Kamei, Y. Koizumi, S. Saito, S. Tanaka, and H. Nishida, "Transmission experiments for UHDTV using 12 GHz band satellite broadcasting," IEICE Technical Report, vol.115, no.287, SAT2015-49, pp.13–16, Oct. 2015.
[14] M. Kamei, M. Nagasaka, S. Nakazawa, and S. Tanaka, "Design of 100-W class GaN power amplifier for on-board SSPA of Ku-band broadcasting satellites," Proc. 33rd AIAA International Communications Satellite Systems Conference, Gold Coast, Australia, AIAA 2015-4346, Sept. 2015.
[15] M. Nagasaka, S. Nakazawa, S. Tanaka, T. Torii, S. Imai, H. Utsumi, M. Kono, K. Yamanaka, and H. Fukumoto, "A Ku-band 100 W power amplifier under CW operation utilizing 0.15 μm GaN HEMT technology," Proc. Asia-Pacific Microwave Conference 2016 (APMC 2016), New Delhi, India, TH2-A-3, pp.1–4, Dec. 2016.
[16] M. Nagasaka, M. Kojima, S. Nakazawa, H. Sujikai, S. Tanaka, T. Torii, H. Utsumi, S. Shinjo, and M. Shimozawa, "120-W Ku-band GaN SSPA with diode linearizer for future broadcasting satellite," Proc. Asia-Pacific Microwave Conference 2018 (APMC 2018), Kyoto, Japan, TH2-D-1, pp.548–550, Nov. 2018.
[17] M. Kojima, M. Nagasaka, Y. Koizumi, S. Nakazawa, A. Iwasaki, Y. Suzuki, K. Saito, and S. Tanaka, "APSK transmission experiments over 12GHz-band satellite channel compared TWTA and SSPA," Proc. 35th AIAA International Communications Satellite Systems Conference, Trieste, Italy, AIAA 2017-5405, Oct. 2017.
[18] Y. Suzuki, K. Tsuchida, Y. Matsusaki, A. Hashimoto, S. Tanaka, T. Ikeda, and N. Okumura, "Performance evaluation of transmission system for 8K Super Hi-Vision satellite broadcasting," Proc. IEEE Global Communications Conference, Austin, the United States, SAC-18-SVC, pp.2928–2933, Dec. 2014.
[19] M. Kojima, M. Nagasaka, Y. Suzuki, Y. Koizumi, K. Saito, and S. Tanaka, "Experimental verification of prototype equalizer for nonlinear compensation over satellite channel," Transactions of Japan Society for Aeronautical and Space Sciences Aerospace Technology Japan, vol.16, no.3, pp.248–253, May 2018.
[20] ARIB STD-B63 ver. 1.6-E1, "Receiver for Advanced Wide Band Digital Satellite Broadcasting," Dec. 2016.
[21] M. Kojima, H. Sujikai, Y. Suzuki, A. Hashimoto, S. Tanaka, T. Kimura, and K. Shogen, "A study on influence of interference of multi-level digital modulations for broadcasting satellite," Transactions of Japan Society for Aeronautical and Space Sciences Aerospace Technology Japan, vol.8, no.ists27, pp.Pj_1–Pj_6, March 2011.
[22] E. Casini, R.D. Gaudenzi, and A. Ginesi, "DVB-S2 modem algorithms design and performance over typical satellite channels," International Journal of Satellite Communications and Networking, vol.22, no.3, pp.281–318, May 2004.
[23] ARIB STD-B44 ver. 2.0-E1, "Transmission system for advanced wide band digital satellite broadcasting," July 2014.
[24] M. Kojima, Y. Koizumi, Y. Suzuki, and H. Sujikai, "Performance comparison of digital pre-distortion techniques over satellite chan-

nel," Proc. IEICE Joint Conference on Satellite Communications, Daejeon, Korea, vol.118, no.237, SAT2018-54, pp.67–71, Oct. 2018.

[25] H. Noto, K. Yamauchi, and M. Nakayama, "Diode linearizer with virtual ground for Ku-band power amplifier," Proc. 2011 IEICE general conference, Tokyo, Japan, C-2-11, p.49, March 2011 (in Japanese).

Masafumi Nagasaka received his B.E. and M.E. degrees in electrical and electronic engineering from Tokyo Institute of Technology, Tokyo, Japan, in 2001 and 2003. He joined Japan Broadcasting Corporation (NHK) in 2003. Since 2008, he has been engaged in research on Ku- and Ka-band satellite broadcasting systems at NHK Science & Technology Research Laboratories. He is currently a senior manager of the Planning & Coordination Division of the laboratories. He received the Young Researcher Award of IEICE in 2011. He is a member of ITE.

Masaaki Kojima received his B.E., M.E., and Ph.D. degrees in electrical and electronic engineering from Tokushima University, Tokushima, Japan, in 2000, 2002, and 2015. He joined Japan Broadcasting Corporation (NHK) in 2002. Since 2006, he has been engaged in research on the non-linear characteristics of broadcasting satellite transponders at NHK Science & Technology Research Laboratories. He is currently a principal research engineer of the laboratories. He received the IEEE CASS Shikoku Chapter Best Paper Award in 2015 and the JC-SAT Award from IEICE in 2017. He is an assistant secretary of the Technical Committee on Satellite Telecommunications of IEICE and a member of ITE and IEEE.

Takuma Torii received his B.E. and M.E. degrees from Tokyo University of Science, Tokyo, Japan, in 2012 and 2014. He joined Mitsubishi Electric Corporation in 2014. Since 2015, he has been engaged in research on Ku-band power amplifiers at Mitsubishi Electric Information Technology R&D Center.

Hiromitsu Utsumi received his B.E. and M.E. degrees in electrical and electronic engineering from Waseda University, Tokyo, Japan, in 1994 and 1996. He joined Mitsubishi Electric Corporation in 1996. Since 1996, he has been engaged in development of high-frequency devices at Mitsubishi Electric Corporation.

Koji Yamanaka received his B.Sc. degree in electric engineering and M.Sc. and Ph.D. degrees in electronic engineering from the University of Tokyo, Japan, in 1993, 1995, and 1998, respectively. In 1998, he joined the Information Technology Research and Development Center, Mitsubishi Electric Corporation, Kamakura, Japan, where he engaged in development of GaAs low-noise monolithic microwave integrated circuit amplifiers and GaN high-power amplifiers. From 2012 to 2018, he managed the Amplifier Group, Mitsubishi Electric Corporation. Currently, he is in charge of the civil application GaN device business section. He is a senior member of IEICE. He was the recipient of the Best Paper Prize of GAAS2005.

Shintaro Shinjo received his B.S. and M.S. degrees in physics and Ph.D. degree in engineering from Keio University, Tokyo, Japan, in 1996, 1998, and 2011. In 1998, he joined Mitsubishi Electric Corporation, Kamakura, Japan, where he has been involved in the research and development of monolithic microwave integrated circuits and solid-state power amplifiers. He is currently a group manager of the Amplifier Group, Microwave Electronics Technology Department. From 2011 to 2012, he was a visiting scholar at the University of California at San Diego, San Diego, CA, USA. He is a senior member of IEEE. He was a recipient of the Prize for Science and Technology (Development Category) of the Commendation for Science and Technology by the Minister of Education, Culture, Sports, Science and Technology in 2009 and the IEICE Electronics Society Award in 2011.

Mitsuhiro Shimozawa received his B.S. and M.S. degrees in electrical engineering from the University of Electro-Communications, Tokyo, Japan, in 1989 and 1991, and the Ph.D. degree in electrical engineering from Tokyo Institute of Technology, Tokyo, Japan, in 2008. He joined Mitsubishi Electric Corporation, Kanagawa, Japan, in 1991, where he has been engaged in research and development of microwave mixers, converters, and transceivers. He was the recipient of the Electronics Society Award of IEICE, Japan, in 2011.

Hisashi Sujikai received his B.E. and M.E. degrees in electrical and electronic engineering from Waseda University, Tokyo, Japan, in 1991 and 1993. From 2013 to 2017, he was a senior manager of the Engineering Administration Department of Japan Broadcasting Corporation (NHK). Since 2017, he has been engaged in research on future satellite broadcasting systems at NHK Science & Technology Research Laboratories. He is currently a senior research engineer of the laboratories. He is a vice chair of the Technical Committee on Satellite Telecommunications of IEICE and a member of ITE.